Doubly *ortho*-linked quinoxaline/triarylamine hybrid as a bifunctional, dipolar electroluminescent template for optoelectronic applications†

Chien-Tien Chen,*[a] Jin-Sheng Lin,[a] Murthy V. R. K. Moturu,[a] Yi-Wen Lin,[a] Wei Yi,[a] Yu-Tai Tao*[b] and Chin-Hsiung Chien[b]

Received (in Cambridge, UK) 9th May 2005, Accepted 14th June 2005
First published as an Advance Article on the web 8th July 2005
DOI: 10.1039/b506409k

The titled hybrid (Q-H) works as a clippable optoelectronic unit. Q-spacer-Q systems function as efficient orange emitters reaching EL intensities (*L*) of up to 6840 cd m^{-2} with η_{ext} of 0.77% and operation efficiencies of 1.60 cd A^{-1} and 0.8 lm W^{-1}. Notably, Q-An acts as a (bluish) green emitter, reaching *L* of 12347 cd m^{-2} with similar operational efficiency.

There has been great interest towards new electroluminescent materials for the fabrication of organic light emitting diodes (OLEDs) owing to their potential applications in large-area flat-panel displays.[1] To optimize device efficiency, balanced charge transport is essential for both carrier types. A logical approach to achieve this is to design dipolar molecular compounds by integrating both ET and HT segments into one component. Dipolar materials framing triarylamine-oxadiazole,[2] triarylamine-pyridine/quinoline,[3] triarylamine-oxadiazole/quinoxaline polymeric and molecular materials have been recently documented.[4]

Notably, the existing dipolar triarylamine-quinoxaline dyads **1** as well as others invoke the 2 : 1 sequential assembly of donor–acceptor fragments through suitable aryl spacers with extended *para*-conjugation, Fig. 1. However, a conceptually different strategy by connecting the individual *ortho*-position of two phenyl rings in diphenylamine framework to the C2–C3 edge of quinoxaline has never been explored. One major merit of this approach is the resultant 1 : 1 hybrid **2** may function as a clippable template to any optoelectronic core units bearing at least one focal point (point of attachment).

Herein, we report the syntheses, single crystal X-ray diffraction structures and optoelectronic properties of iminostilbene-based triaryl amines with fused quinoxaline along its C9–C10 edge as bi-functional dipolar materials (QLIMS) promising for applications in OLEDs as efficient green and orange emitters.[5]

The requisite clippable **Q**LIMS-H (**Q**-H, **2a**) can be readily prepared in four steps from iminostilbene.† Preliminary searches for suitable functional aryl pendant groups, spacers, and cores led to the optimal subclass as shown in Scheme 1. These desired molecular materials, **Q**-Ar (**2b–c**) and **Q**-spacer-**Q** (**3a–b**), were synthesized in 70–87% yields by direct aromatic C–N bond formation[6] of **Q**-H (**2a**)† with respective phenyl and 9-anthryl halides, 4,4′-diiodo-1,1′-biphenyl, and 3,6-dibromo-9,9-diphenylfluorene by using catalytic $Pd_2(dba)_3$ and $P(t\text{-}Bu)_3$ (in a 1/3 mol% ratio) in the presence of sodium *tert*-butoxide (3 equiv) in refluxing toluene for 8 h as illustrated in Scheme 1.

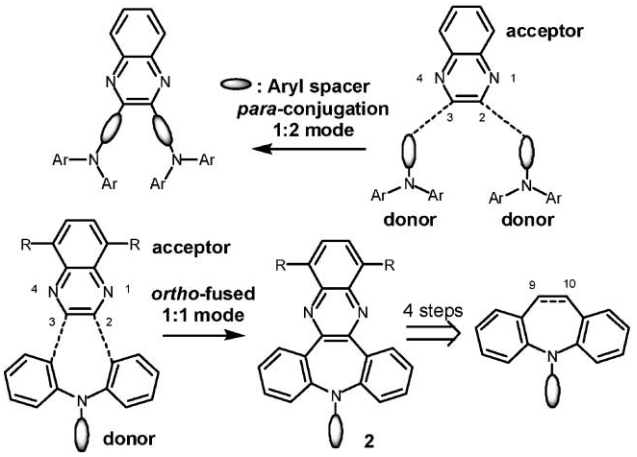

Fig. 1 Two different strategies in assembling quinoxaline and diarylamine units to form integrated, dipolar molecular OLED materials.

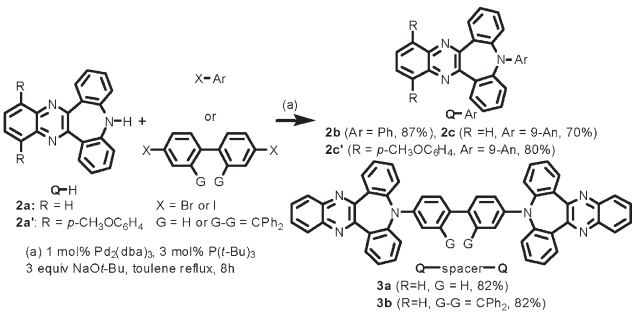

Scheme 1 Clipping of **Q**-H (**2a**) to aryl, biphenyl, and fluorene cores.

The structural features of **Q**-Ar (**2a–c**) and **Q**-spacer-**Q** (**3a–b**) were resolved spectroscopically and further proven by X-ray crystallographic analyses. The complete orthogonal feature in **2c** (Fig. 2a) prevents the unfavorable steric interaction of the pendant anthryl group with the flanking phenyl rings in the iminostilbene template, resulting in increased charge transfer (CT) from the nitrogen lone pair to the quinoxaline backbone. The structural features of **3a** (Fig. 2a) and **3b** are similar to that of **2b** (Ar = Ph) but display unusual ladder-type structures with anti-parallel

[a]*Department of Chemistry, National Taiwan Normal University, #88, Sec. 4, Ding-jou Road, Taipei, 11650, Taiwan, ROC. E-mail: chefv043@scc.ntnu.edu.tw; Fax: +886 2 2932 4249; Tel: +886 2 2930 9095*
[b]*Institute of Chemistry, Academia Sinica, 106, Taipei, Taiwan, ROC*
† Electronic supplementary information (ESI) available: Experimental details of compounds **2a–c** and **3a,b**, UV-Vis, PL, CV spectra, *I-V-L* characteristics and EL spectra of devices, ORTEP drawings, and selected crystal data for **2c**, **3a**, and **3b**. See http://dx.doi.org/10.1039/b506409k

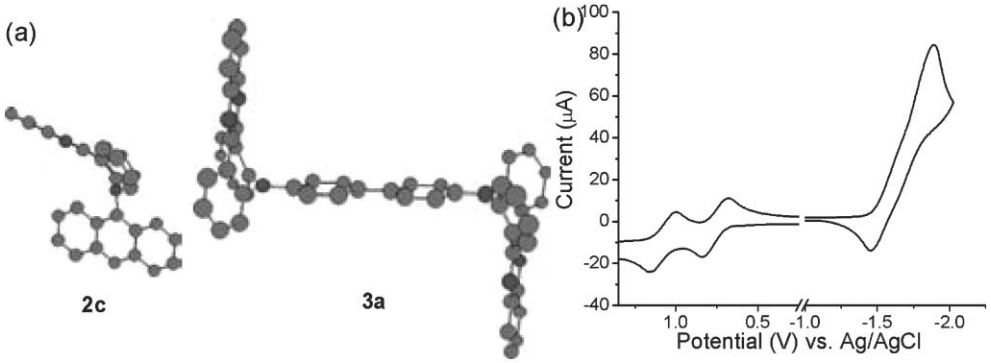

Fig. 2 Chem 3D presentations (all hydrogens omitted, side view) for the X-ray crystal structures of **2c** and **3a** (left). Cyclic voltammogram of compound **3a** with 0.1 M n-Bu_4NClO_4 in $CHCl_3$ (right).

arrangement of the two quinoxaline backbones.[7] On the other hand, the negligible CT absorption band observed in **2b** (**Q**-Ph) may have to do with the facile delocalization of the iminostilbene nitrogen lone pair to the pendent phenyl ring, Table 1.

All these molecular materials show bluish green (**2c** and **2c′**, 501 nm), green (**2a**, 526 nm), yellowish green (**2b**, 558 nm), and orange fluorescent emissions (**3a** and **3b**, 590–600 nm) in solution upon UV excitations, respectively. In all cases except **2c** and **2c′**, the absorption and emission bands (λ_{max}) display progressive bathochromic shifts (from **2b** to **3a,b**) due to the increased extent (for **3a**) or enforced rigidity (for **3b**) of π-conjugation. In addition, the full width at half maximums (*fwhm*) for **2b, 3a**, **a**nd **3b** lie in the range of 98–129 nm, Table 1. In marked contrast, a much narrower emission band resulted in the case of **2c** (*fwhm* = 64 nm), indicating its unique rigidity and reduced conformational change in excited state.

These compounds showed excellent thermal stability with glass transition temperatures exhibited from 86–154 °C for **Q**-Ar and 202–294 °C for **Q**-spacer-**Q** systems. The remarkable jump in T_g by 68 °C (from **2b** to **2c**) and 92 °C (from **3a** to **3b**) was attributed to the orthogonal feature associated with **2c** and **3b**.† The drastic change in T_g by 92 °C by changing the spacer from biphenyl to 9,9-diphenylfluorenyl is remarkable (the difference is only 19 °C between **4**[8] and **6**[9]). Notably, clipping **Q**-H to these two spacers is beneficial in improving the morphological stability of the resultant materials as compared to compounds (**4** and **6**) having iminostilbenyl and diarylamino peripheral groups. In comparison, the T_g for **6** (with 9,9-diarylfluorene spacer) showed in the range of 97–129 °C[9] and the T_g for **4** (with biphenyl spacer) exhibited in the range of 60–152 °C.[8,10] In addition, the T_g (154 °C) of **2c** ($C_{34}H_{21}N_3$, fw: 471.6) is significantly higher than common hole-transporting materials of even larger molecular size such as 1,4-bis-(1-naphthylphenylamino)-biphenyl-**5** ($C_{44}H_{32}N_2$, fw: 588.7, T_g = 95 °C) and 1,4-bis-(phenyl-*m*-tolylamino)biphenyl ($C_{38}H_{32}N_2$, fw: 516.3, T_g = 60 °C),[11] supporting the concept of our unique molecular design.

The redox behaviors of these compounds were evaluated by cyclic voltammetry (CV) experiments at ambient temperature, Table 1. The similar or even lower reduction potentials (−1.56 to −1.94 V) of the **Q**-Ar series compared to the parent diarylquinoxaline[12] and the 2 : 1 mode system[4a,b] (−1.81 to −2.17 V, Fig. 1) indicate the quinoxaline backbone in **Q**-Ar can retain its electron-accepting nature even by the incorporation of the HT, triarylamino moiety in a rigid doubly *ortho*-linked mode. In compounds **3a** and **3b** two reversible oxidation redox couples were observed† and were attributed to the sequential electrochemical oxidations occurring at either central nitrogen of the peripheral **Q** units. The cyclic voltammogram for **3a** reveals its dipolar nature of the new materials system, involving two-electron oxidation and two-electron reduction (Fig. 2b). Notably, between the two

Table 1 Optical, morphological, and electrochemical data for Q–Ar (**2a–c**) and Q-spacer-Q (**3a–b**)

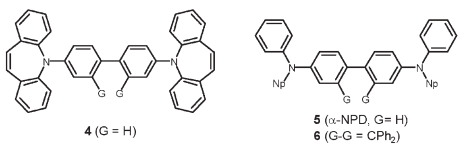

Cpd	λ_{max}[a] (ε), nm	λ_{max},[a] nm	Φ_f,[a] %	T_g/T_d, °C	E,[b] V
2a	352 (6677) 397 (8397)	526 (74[c])	29.7	57/256	−1.78
2b	352 (9188) 399 (1485)	558 (98)	3.1	86/273	−1.69
2c	372 (10626) 419 (11914)	501 (64)	2.6	154/350	−1.61, −1.94[e]
2c′	409 (24267)	502 (74)	7.0	159/464	−1.56
3a	328 (15151) 423 (1042)	589[d] (109)	3.2[d]	202/467	0.76, 1.07, −1.71
3b	344 (41293) 444 (3628)	600[d] (129)	2.3[d]	294/470	0.38, 0.76
4	300, 340	530 (—)	—	110/—	0.70[f]
6	352, 379	457	15	129/—	0.69, 1.04[g]

[a] Measured in CH_2Cl_2 unless otherwise stated. [b] Measured in $CHCl_3$. [c] The data in parentheses correspond to full-width at half-maximum (*fwhm*). [d] Measured in toluene. [e] Measured in THF. [f] Ref. 8. [g] Ref. 9.

Table 2 Electroluminescence data for the compounds **2a–c** and **3a–b**

Config.[a]	*Em.* λ_{max}, nm	V_{on},[b] V	η_{ext},[c] %	η_c,[c] cd A^{-1}; η_p,[c] lm W^{-1}	*L*,[d] cd m^{-2}
A (**2b**)	522/524 (90[e])	3.0 (5.5[f])	0.22	0.74[f]; 0.43[f]	2740 (585[g])
D (**2c**)	510/504 (62)	3.0 (5.4[f])	0.55	1.45; 0.84	11623 (293[f])
B (**2c**)	510/506 (64)	3.8 (7.0[f])	0.55	1.70; 0.76	9542 (340[f])
B (**2c′**)	518/518 (74)	6.2 (9.1[f])	0.58	1.97; 0.68	12347 (400[f])
C (**3a**)	600/604 (100)	3.3 (6.3[f])	0.77	1.60; 0.80	6840 (319[f])
B (**3b**)	604/600 (110)	4.0 (6.9[f])	0.58	1.22; 0.56	7273 (243[f])

[a] Device configuration A: ITO/BPAPF(40 nm)/**2b**(40 nm)/Mg(Ag), B: ITO/**2c** or **3b**(40 nm)/BCP(10 nm)/Alq_3(40 nm)/Mg(Ag), C: ITO/**3a** (40 nm)/BCP(10 nm)/TPBI(40 nm)/Mg(Ag), D: ITO/**2c** (40 nm)/TPBI (40 nm)/Mg(Ag). [b] Turn on voltage. [c] External quantum efficiency (η_{ext}), current efficiency (η_c), and power efficiency (η_p). were measured at 20 mA cm^{-2}. [d] Maximum brightness. [e] The data in parentheses correspond to the full-width at half-maximum. [f] Measured at 20 mA cm^{-2}. [g] Luminance measured at 100 mA cm^{-2}.

9,9-diphenylfluorene-based materials (**3b** and **6**) in Table 1, **3b** shows lower oxidation potential (ΔE_{ox1} = 0.31 V). It also tends to get oxidized easier than **3a** and **4** bearing the biphenyl spacer (ΔE_{ox1} = 0.32–0.38 V).

These compounds were subjected to optoelectronic studies by first fabricating bilayer OLEDs with a device configuration of ITO/BPAPF(40 nm)/**2a–c**(40 nm)/Mg : Ag, where **Q**-Ar (**2a–2c**) acts as ET and emitting layer and BPAPF[13a] serves as HT materials. Their green emitting EL efficiencies were unsatisfactory. Among them, **Q**-Ph (**2b**) led to the best device performance and exhibits maximum EL brightness (*L*) of 2740 cd m^{-2} and an operational brightness of 585 cd m^{-2} at 100 mA cm^{-2} with external quantum efficiency (η_{ext}) of 0.22%, Table 2. The devices (luminance-η_c and power-η_p) efficiencies for this device at 100 mA cm^{-2} are 0.74 cd A^{-1} and 0.43 lm W^{-1}, respectively.† Although the device characteristics were taken with the unsealed device and the device optimization was not attempted, the device performance for **2b** remains 10 times better than dipolar type ET and emitting materials to date.[14]

The HT and emitting properties of **Q**-Ar and **Q**-spacer-**Q** were further examined by applying a device structure of ITO/**Q** family(40 nm)/Alq_3 or TPBI (40 nm)/Mg : Ag, where Alq_3 and TPBI serve as ET materials.[13b,c] In all cases, the minor undesired emission leakage (*i.e.*, entry 2, Table 2) presumably due to faster HT attributes of **Q** family was avoided by inserting a 10 nm BCP layer between **Q** family and ET layers.[13d] The maximum brightness for orange-emitting **3a** and **3b** reached 6840 and 7273 cd m^{-2} with η_{ext} of 0.77 and 0.58%, respectively, in conjunction with the BCP hole-blocker (Table 2). In comparison with **3b**, slightly better working efficiencies and performance were observed for **3a** under 20 mA cm^{-2} working conditions. Notably, the device efficiency for **3a** which functions as a HT and emitter seems better than those for **4** (4,4′-bis(*N*-iminostilbenyl)biphenyl, ISB) and IDB (4,4′-bis-*N*-iminodibenzyl) acting as HT materials in conjunction with Alq_3 as ET and emitting layer in terms of maximum *L* (6840 *vs* 11,200 and 600 cd m^{-2} at 5 mA cm^{-2}), V_{on} (3.3 *vs* 9.0 V, 12.9 at 5 mA), power efficiency (0.80 *vs* 0.16 and 0.025 lm W^{-1} at 5 mA) and η_{ext} (0.77 *vs* 0.62 and 0.15%).[8]

Finally to our surprise, **2c** ($C_{34}H_{21}N_3$, fw: 471.6) and **2c′** may also function as an ET and (bluish) green emitter, leading to 9542 and 12347 cd m^{-2} maximum brightness, V_{on} of 3.8 V, η_c of 1.70–1.97 cd A^{-1}, and η_p of 0.68–0.76 lm W^{-1} at 20 mA cm^{-2} conditions. The resultant tri-layer device retains its sharpest emission (*fwhm* = 62 nm) as that in solution. Compact, dipolar materials like **2c** with spiral molecular shape and exhibits unique photophysical and optoelectronic properties was unprecedented, auguring well for its potential applications and the use of **Q**-H as a clippable optoelectronic template.

Notes and references

1 L. S. Hung and C. H. Chen, *Mater. Sci. Eng. Report*, 2002, **39**, 143.
2 (*a*) H. Mochizuki, T. Hasui, M. Kawamoto, T. Shiono, T. Ikeda, C. Adachi, Y. Taniguchi and Y. Shirota, *Chem. Commun.*, 2000, 1923; (*b*) N. Tamoto, C. Adachi and K. Nagai, *Chem. Mater.*, 1997, **9**, 1077; (*c*) Z. H. Peng, Z. N. Bao and M. E. Galvin, *Chem. Mater.*, 1998, **10**, 2086.
3 (*a*) Y. Liu, H. Ma and A. K.-Y. Jen, *Chem. Commun.*, 1998, 2747; (*b*) Y. Z. Wang and A. J. Epstein, *Acc. Chem. Res.*, 1999, **32**, 217; (*c*) S. A. Jenekhe, L. D. Lu and M. M. Alam, *Macromol.*, 2001, **34**, 7315.
4 (*a*) K. R. J. Thomas, J. T. Lin, Y.-T. Tao and C.-H. Chuen, *Chem. Mater.*, 2002, **14**, 3852; (*b*) J. Kido, G. Harada and K. Nagai, *Chem. Lett.*, 1996, 161; (*c*) S.-Y. Song, M. S. Jang, H.-K. Shim, D.-H. Hwang and T. Zyung, *Macromol.*, 1999, **32**, 1482.
5 For the uses of the corresponding carbocycle analogs (*i.e.*, dibenzosuberane) in catalysis, see: (*a*) C.-T. Chen, S.-D. Chao, K.-C. Yen, C.-H. Chen, I.-C. Chou and S.-W. Hon, *J. Am. Chem. Soc.*, 1997, **119**, 11341; (*b*) C.-T. Chen, S.-D. Chao and K.-C. Yen, *Synlett*, 1998, 924; (*c*) C.-T. Chen and S.-D. Chao, *J. Org. Chem.*, 1999, **64**, 1090. In LC optical switches, see: (*d*) C.-T. Chen and Y-C. Chou, *J. Am. Chem. Soc.*, 2000, **122**, 7662.
6 J. F. Hartwig, *Acc. Chem. Res.*, 1998, **31**, 852.
7 CCDC 271944-271946. See http://dx.doi.org/10.1039/b506409k for crystallographic data in CIF or other electronic format.
8 (*a*) B. E. Koene, D. E. Loy and M. E. Thompson, *Chem. Mater.*, 1998, **10**, 2235; (*b*) D. F. O'Brien, P. E. Burrows, S. R. Forrest, B. E. Koene, D. E. Loy and M. E. Thompson, *Adv. Mater.*, 1998, **10**, 1108.
9 K.-T. Wong, Z.-J. Wang, Y.-Y. Chien and C.-L. Wang, *Org. Lett.*, 2001, **3**, 2285.
10 H. Tanaka, S. Tokito, Y. Taga and A. Okada, *Chem. Commun.*, 1996, 2175.
11 K. Naito and A. Miura, *J. Phys. Chem.*, 1993, **97**, 6240.
12 M. J. Edelmann, J.-M. Raimundo, N. F. Utesch, F. Diederich, C. Boudon, J.-P. Gisselbrecht and M. Gross, *Helv. Chim. Acta*, 2002, **85**, 2195.
13 BPAPF: 9,9-bis{4-[di-(*p*-biphenyl)aminophenyl]}fluorene. For its application as a HT materials, see: (*a*) C.-W. Ko and Y.-T. Tao, *Synth. Met.*, 2002, **126**, 37; (*b*) Alq_3: tris-(8-quinolinato)aluminum; (*c*) TPBI: 1,3,5-*t*ris-(*N*-*p*henyl-*b*enzimidazole-2-yl)benzene; (*d*) BCP: 2,9-dimethyl-4,7-diphenyl-1,10-phenanthroline.
14 (*a*) *L* = 200 cd m^{-2} with η_{ext} of 0.11% for quinoxaline-based oligomers: M. Jandke, P. Strohriegl, S. Berleb, E. Werner and W. Brütting, *Macromol.*, 1998, **31**, 6434; (*b*) See also: T. Yamamoto, K. Sugiyama, T. Kushida, T. Inoue and T. Kanbara, *J. Am. Chem. Soc.*, 1996, **118**, 3930.

